

**Thermal decomposition and Fourier transform infrared spectroscopic study of manganese hypophosphite monohydrate ( $Mn(H_2PO_2)_2 \cdot H_2O$ ), ammonium manganese phosphate monohydrate ( $NH_4MnPO_4 \cdot H_2O$ ) and deuterated analogues**

การศึกษาการสลายตัวด้วยความร้อน และ สเปกตราราฟิเรียร์ทรานสฟอร์มอินฟราเรด ของแมงกานีสไฮโปฟอสไฟต์โมโนไฮเดรต แอมโมเนียมแมงกานีสฟอสเฟตโมโนไฮเดรต และ สารประกอบในรูปดิวเทอเรต

Pittayagorn Noisong (พิทยากรณ์ น้อยทรงค์)\*

Dr.Chanaiporn Danvirutai (ดร. ไฉนพร ด่านวิรุทัย) \*\*

Dr. Tipaporn Srithanratana (ดร. ทิพาภรณ์ ศรีธัญรัตน์) \*\*

**ABSTRACT**

The manganese hypophosphite monohydrate ( $Mn(H_2PO_2)_2 \cdot H_2O$ ), ammonium manganese phosphate monohydrate ( $NH_4MnPO_4 \cdot H_2O$ ) and their deuterated analogues were synthesized. Thermal decomposition of these compounds were reported for the first time. The TGA and DSC data indicated two mass loss steps at 120-180 °C and 330-370 °C for  $Mn(H_2PO_2)_2 \cdot H_2O$ , while three mass loss steps were observed for  $NH_4MnPO_4 \cdot H_2O$ . The interesting point was, the final products of the two titled compounds was  $Mn_2P_2O_7$ . The FTIR spectra were assigned based on the factor group splitting analysis. New band appear at 1384  $cm^{-1}$  was first observed in  $Mn(H_2PO_2)_2 \cdot H_2O$  and attributed to the very low bending mode of water molecule. The wagging libration at the 740  $cm^{-1}$  was clearly observed in  $NH_4MnPO_4 \cdot H_2O$ .

**บทคัดย่อ**

ได้สังเคราะห์สารประกอบ แมงกานีสไฮโปฟอสไฟต์โมโนไฮเดรต ( $Mn(H_2PO_2)_2 \cdot H_2O$ ) แอมโมเนียมแมงกานีสฟอสเฟตโมโนไฮเดรต ( $NH_4MnPO_4 \cdot H_2O$ ) และสารประกอบดิวเทอเรต การสลายตัวทางด้านความร้อนของสารเหล่านี้ รายงานเป็นครั้งแรก ข้อมูลทีจีเอ และ ดีเอสซี แสดงให้เห็นถึงการสลายตัวสองขั้นตอน ที่ 120-180 °C และ 330-370 °C สำหรับ  $Mn(H_2PO_2)_2 \cdot H_2O$  ในขณะที่ได้สังเกตเห็นการสลายตัวสามขั้นตอนสำหรับ  $NH_4MnPO_4 \cdot H_2O$  จุดที่น่าสนใจ คือ ผลิตภัณฑ์สุดท้ายของการสลายตัวของสารทั้งสองนี้คือ  $Mn_2P_2O_7$  สเปกตรัมเอฟทีไออาร์จัดประเภทได้โดยอาศัยการวิเคราะห์การแตกออกของแฟกเตอร์กรุป ได้สังเกตเห็นแถบใหม่ที่ 1384  $cm^{-1}$  เป็นครั้งแรก และเป็นการสั่นแบบโค้งงอที่ค่าต่ำมากของโมเลกุลน้ำ ไลเบรชันแบบเวกกิงที่ 740  $cm^{-1}$  สังเกตเห็นได้ชัดเจนใน สาร  $NH_4MnPO_4 \cdot H_2O$

**คำสำคัญ :** เอฟทีไออาร์ แมงกานีสไฮโปฟอสไฟต์โมโนไฮเดรต แอมโมเนียม แมงกานีสฟอสเฟตโมโนไฮเดรต

**Key Words :** FTIR,  $Mn(H_2PO_2)_2 \cdot H_2O$ ,  $NH_4MnPO_4 \cdot H_2O$

\* Master student, Master of Science in Physical Chemistry, Department of Chemistry, Faculty of Science, Khon Kean University.

\*\* Asst.Prof. Department of Chemistry, Faculty of Science, Khon Kaen University, Advisor.

## 1. Introduction

Inorganic phosphate hydrates were transformed to various forms of phosphates or polyphosphates through the dehydration and hydrolysis reactions upon heating (Onoda et al, 2002, Onoda et al, 2006). They were cyclo-phosphate, polyphosphates and ultraphosphate in a group of condensed phosphates (Onoda et al, 2006). Pyrophosphate was the simplest condensed phosphate. Phosphates have been used a various applications such as ceramic materials, catalysts, fluorescent materials, dielectric substances, metal surface treatment, manure, detergent, food additives, fuel cells, pigment, etc (Onoda et al, 2001, Onoda et al, 1999). Metal pyrophosphate have been used in the field of luminescence and biomaterials ( $\text{Ca}_2\text{P}_2\text{O}_7$ ) (Bian et al, 2003), industrial catalyst ( $(\text{VO})_2\text{P}_2\text{O}_7$ ) (Smaalen et al, 2005). Therefore, they were of great interest to be selected for studying their chemical and physical properties. The interesting point, the thermal final decomposition product of various manganese phosphate hydrates was  $\text{Mn}_2\text{P}_2\text{O}_7$  compound, e.g.  $\text{Mn}(\text{HPO}_3)$  (Chung et al, 2005),  $\text{MnPO}_4 \cdot \text{H}_2\text{O}$  (Boonchom et al, 2007). The phosphate oxo-anions such as  $(\text{PO}_4)^{3-}$ ,  $(\text{P}_2\text{O}_7)^{4-}$  were species of next generation positive-electrode materials for lithium batteries and offered additional advantages in practical applications due to their lower cost, safety, benign environmental properties stability and low toxicity (Julien et al, 2006). The manganese hypophosphite monohydrate plays a critical role in the manufacture of nylon carpet fibers, improves fiber's UV stability and dye color fastness(nylon fiber), primary chemical intermediate for the production of various products (pharmaceuticals) and in the preparation of certain linear condensation

polymers (chemical intermediate)(<http://www.crowid.org/rchiverhodium/pdf/hypophosphoric.pdf>).

In addition, in the presence of catalysts such as palladium, copper and platinum black, hydrated hypophosphite salts generates hydrogen gas, where one H in each  $\text{H}_2$  molecule comes from water and the other comes from hypophosphite (Marincean et al, 2005). This behavior may be important for the water gas shift reaction.

In the last two decades, metal hypophosphite compounds were synthesized (Marcos et al, 1992). Isolated hypophosphite anions had been studied using quantum mechanicals calculations in 1996 (Liu et al, 1996). Zachariasen and Mooney (Zachariasen & Mooney, 1934) reported that this anion belonged to a  $C_{2v}$  symmetry structure. Zinc hypophosphite monohydrate ( $\text{Zn}(\text{H}_2\text{PO}_2)_2 \cdot \text{H}_2\text{O}$ ) (Tanner et al, 1997) and rare earth hypophosphites (Tanner et al, 1999) were reported on the crystallographic and spectroscopic data. Marcos et al., published the synthesis of the Mn(II)-hypophosphite anion system in three different hydrates ( $\text{Mn}(\text{H}_2\text{PO}_2)_2 \cdot n\text{H}_2\text{O}$ ,  $n = 1, 2, 3$ ). In the case of  $\alpha\text{-Mn}(\text{H}_2\text{PO}_2)_2 \cdot \text{H}_2\text{O}$ , only crystal structure and magnetic properties were reported. This compound existed in two polymorphs and was isostructural with zinc hypophosphite. According to the literature, the  $\alpha\text{-Mn}(\text{H}_2\text{PO}_2)_2 \cdot \text{H}_2\text{O}$  compound crystallized in the monoclinic space group  $P2_1/c$  ( $C_{2h}^5$ ) with  $Z = 4$ ,  $a = 7.8601(3) \text{ \AA}$ ,  $b = 7.4411(3) \text{ \AA}$ ,  $c = 10.7717 \text{ \AA}$  and  $\beta = 102.859^\circ(2)$ . The fundamental vibrational modes under  $C_{2v}$  point group of hypophosphite anions structure and deuterated analogue were summarized by Liu et al. Some physical properties data of this hydrate such as the thermal decomposition and IR spectra have not been

reported elsewhere. Therefore this paper focuses on studying of these physical properties.

Dittmarite was reported to be a biomineral and found (rather infrequently) in urinary calculi (Šoptrajanov et al, 2002). The well known series of compounds of type  $M^I M^{II} PO_4 \cdot H_2O$  ( $M^I = K^+, NH_4^+$ ;  $M^{II} = Mn^{2+}, Fe^{2+}, Co^{2+}, Ni^{2+}$ ) related to the dittmarite. All of these compounds were crystallized in the rhombic space group  $P_{mn}2_1(C_{2v}^7)$  with  $Z = 2$  (Carling et al, 1995). Furthermore, the saline soil in Northeast Thailand was one cause of the precipitation of iron and manganese phosphate and spurs the ferrolysis process. Important factors effecting rice yields in the Northeast Thailand were the precipitations of iron and manganese compounds that changed the physical properties of soil (Danvirutai et al, 1989).

In this paper, the thermal decomposition of  $Mn(H_2PO_2)_2 \cdot H_2O$  and  $NH_4MnPO_4 \cdot H_2O$  were described, which have not been reported elsewhere. The final thermal product of these hydrates was  $Mn_2P_2O_7$ . The FTIR spectra of these compounds and their deuterated analogue were studied. The correlation field splitting analysis of hypophosphite was first suggested. The interesting observation was the appearance of new band at  $1384\text{ cm}^{-1}$  in both protiated and deuterated hypophosphite, had never been observed and reported before. In the region of  $2270\text{-}1990\text{ cm}^{-1}$ , several weak bands were observed and will be discussed.

## 2. Experimental

### 2.1 Preparation

The manganese hypophosphite monohydrate was synthesized by the method reported by Marcos and co-worker. Acetone (40 mL, 99.8 %, Carlo erba) was added to an aqueous solution (15mL) containing

10 g  $Mn(NO_3)_2 \cdot 4H_2O$  (97 % PRS panreac) and 4 mL  $H_3PO_2$  (50%, Sigma Aldrich). The obtained suspension was heated for 10 min at the boiling temperature of acetone. A light pink precipitate was separated from the mother liquor by filtration, washed with acetone (three time) and air dried. The deuterated analogue was prepared by the same procedure in partially deuterated (80-90%  $D_2O$ ) solvent.

The Ammonium salts ( $NH_4MnPO_4 \cdot H_2O$ ) was prepared by using a method reported by Bassett and Bedwell (Basset & Bedwell, 1993). A 0.5 M solution of  $MnCl_2 \cdot 4H_2O$  was added to an excess saturated  $(NH_4)_2HPO_4$  solution (10M). The resulting precipitate was digested at  $85 \pm 5\text{ }^\circ\text{C}$  for 1-2 days, after that the product was filtered, washed with DI water and dried in a desiccators. In the preparation of this salt, hydrazonium sulfate,  $(N_2H_6)SO_4$  was added in order to prevent aerobic oxidation of the divalent metal ion under the extremely basic condition. Deuterated analogue of the ammonium manganese phosphate hydrate was prepared by the method described for the hydrogenous compounds with several modifications by using  $D_2O$  as solvent.

### 2.2 Characterization

The manganese content in each hydrate was determined by using atomic absorption spectrophotometry (AAS, Perkin Elmer Analyst 100). The water content was analyzed by TG data. The infrared spectra were recorded using KBr pellets on Perkin Elmer spectrum GX FTIR/FT Raman spectrophotometer with 16 scans, in the range of  $4000\text{-}370\text{ cm}^{-1}$ . The working resolution of the instrument was  $4\text{ cm}^{-1}$ . The FTIR spectrum of the calcined product of hydrate compounds were recorded. Thermogravimetric (TG) and differential

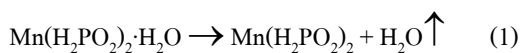
scanning calorimetric curves were carried out for samples (5-10 mg) in aluminum crucibles, in the temperature range of 30-400 °C using Perkin Elmer Pyris Diamond thermogravimetric analyzer and Perkin Elmer Pyris one, respectively. The heating rate employed was 10 °C /min.

### 3. Results and discussion

#### 3.1 Thermal decomposition

The DSC curve of  $\text{Mn}(\text{H}_2\text{PO}_2)_2 \cdot \text{H}_2\text{O}$  (Fig. 1) appears two endothermic peaks at 151.46 °C and 360.82 °C (maximum peak, on set peak at 142.34 °C, 356.00 °C, respectively) are due to the dehydration and decomposition of this compound, respectively. The typical properties of manganese hypophosphite at the temperature 150 and over 350 °C correspond to the dehydration and decomposition of this compound, respectively. The TG/DTG curves of this compound obtained under nitrogen atmosphere from 30 – 400 °C are presented in Fig. 2. The thermal decomposition behavior shows two steps in the temperature range from 120 to 400 °C. The experimental mass loss of water in  $\text{Mn}(\text{H}_2\text{PO}_2)_2 \cdot \text{H}_2\text{O}$  is 8.36 % which corresponds well with the theoretical mass loss of 8.87 %. The experimental mass loss over the 330-370 °C temperature range is attributed to the decomposition reaction. The mechanism for the thermal decomposition of manganese hypophosphite monohydrate can be suggested as follow:

Step 1 (in the range of 120-180 °C )



The enthalpy change of dehydration in this step is found to be 337.220 J/g.

Step 2 (in the range of 330-370 °C)

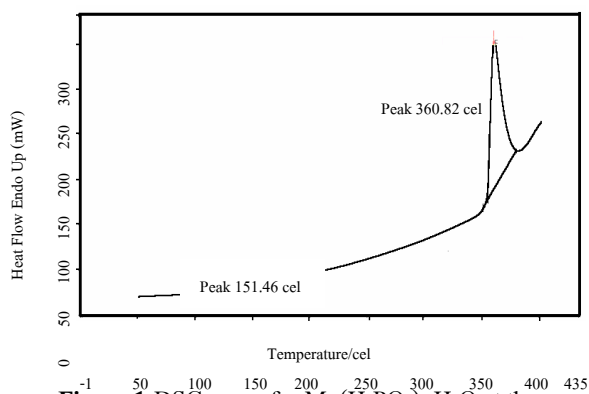
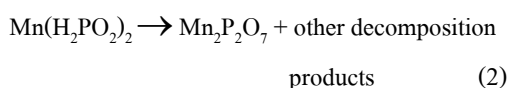


**Figure 1** DSC curve for  $\text{Mn}(\text{H}_2\text{PO}_2)_2 \cdot \text{H}_2\text{O}$  at the heating rate 10 °C/min .

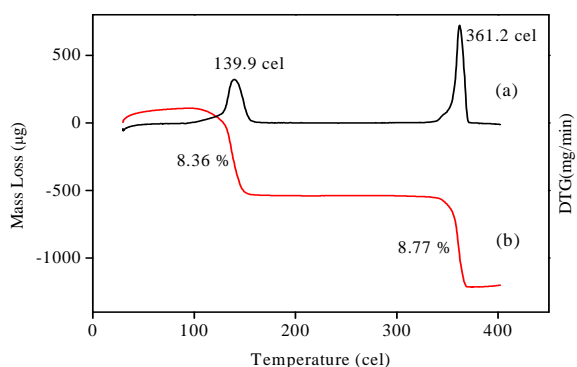


**Figure 2** DTG (a) and TG (b) curves of  $\text{Mn}(\text{H}_2\text{PO}_2)_2 \cdot \text{H}_2\text{O}$  compound at the heating rate 10 °C/min in  $\text{N}_2$  atmosphere.

This step represents the decomposition of manganese hypophosphite compound and the enthalpy change is found to be 1952.301 J/g. The result from TG and DSC methods of hypophosphite compound confirm that the dehydration process occurs at about 140 °C, while the decomposition occurs at 360 °C.

The TG/DTG and DSC curves of  $\text{NH}_4\text{MnPO}_4 \cdot \text{H}_2\text{O}$  are shown in Figure 3 and 4, respectively. The thermal decomposition of this compound exhibits three steps of mass loss, however step 1 and 2 are coupled of mass losses. The mechanism for the thermal decomposition of this compound is suggested as follow:

Step 1, 2 ( in the range of 100-350 °C )



Step 3 (in the range of 350-550 °C)

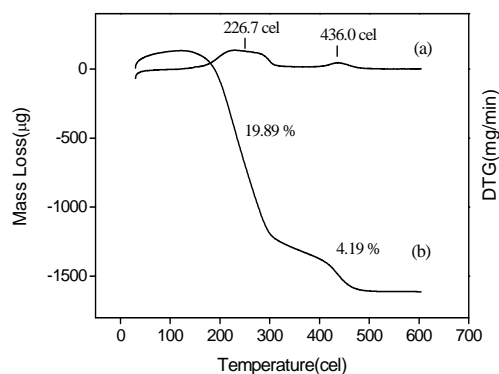
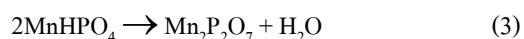


**Figure 3** DTG (a) and TG (b) curves of  $\text{NH}_4\text{MnPO}_4 \cdot \text{H}_2\text{O}$  compound at the heating rate  $10^\circ\text{C}/\text{min}$  in  $\text{N}_2$  atmosphere.

The DSC curve of this compound provides the enthalpy change of step 1, 2 to be  $494.304 \text{ J/g}$ , whereas for step 3, the value can not be reported due to the upper temperature is higher than the instrument limit. The calcined product of  $\text{Mn}(\text{H}_2\text{PO}_2)_2 \cdot \text{H}_2\text{O}$  at  $450^\circ\text{C}$  and  $\text{NH}_4\text{MnPO}_4 \cdot \text{H}_2\text{O}$  at  $550^\circ\text{C}$  is confirmed from FTIR spectrum (Fig. 5).

### 3.2 Infrared spectra

The FTIR spectra of  $\text{Mn}(\text{H}_2\text{PO}_2)_2 \cdot \text{H}_2\text{O}$  and its deuterated analogue are presented in Fig. 6 and FTIR spectra of manganese hypophosphite anhydrous are shown in Fig. 7. The band assignments for the IR spectra of this compound are summarized in Table 1. The vibrational spectrum  $\text{NH}_4\text{MnPO}_4 \cdot \text{H}_2\text{O}$  and its deuterated analogue compound are shown in Fig. 9.

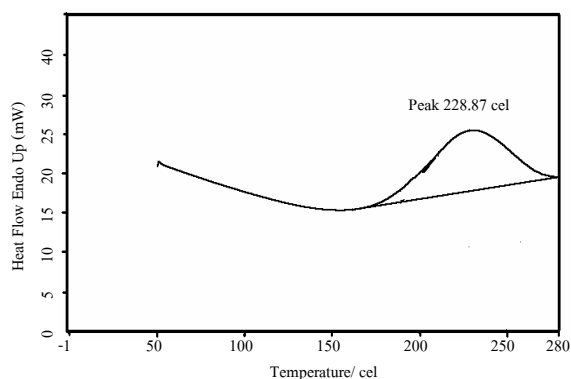


**Figure 4** DSC curve of  $\text{NH}_4\text{MnPO}_4 \cdot \text{H}_2\text{O}$  at heating rate  $10^\circ\text{C}/\text{min}$ .

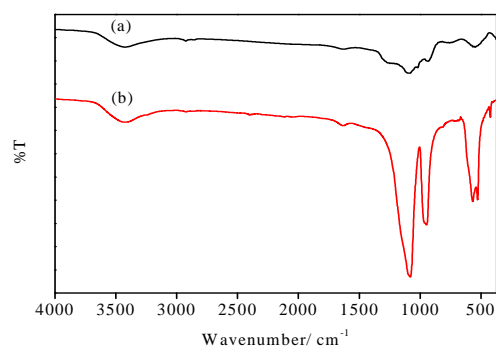


**Figure 5** FTIR spectra of  $\text{Mn}(\text{H}_2\text{PO}_2)_2 \cdot \text{H}_2\text{O}$  calcined at  $450^\circ\text{C}$  (a) and  $\text{NH}_4\text{MnPO}_4 \cdot \text{H}_2\text{O}$  at  $550^\circ\text{C}$  (b).

#### 3.2.1 $\text{Mn}(\text{H}_2\text{PO}_2)_2 \cdot \text{H}_2\text{O}$

A free  $\text{H}_2\text{O}$  molecule possesses  $C_{2v}$  symmetry. There are three normal modes of vibration namely,  $\nu_1(A_1)$ ,  $\nu_2(A_1)$  and  $\nu_3(B_2)$  of which  $\nu_1$  and  $\nu_3$  are stretching and  $\nu_2$  is bending vibrations. Three infrared and three Raman active bands are expected from a  $\text{H}_2\text{O}$  molecule, but three bands are observed in the FTIR spectra of this compounds in the stretching region of water molecules. Because of the lowering site symmetry of the  $\text{H}_2\text{O}$  molecules in the lattice to get with the correlation field splitting, the number of bands are observed including bands due to the combinations, overtone and Fermi resonance.

Correlation field splitting of  $\text{H}_2\text{O}$  in  $\text{Mn}(\text{H}_2\text{PO}_2)_2 \cdot \text{H}_2\text{O}$  were analyzed base on the point

group ( $C_{2v}$ ), site group ( $C_1$ ) and unit cell symmetry (space group)  $C_{2h}^5$ . The number of fundamental modes are :

$$\Gamma(\text{vib}, \text{H}_2\text{O}) = 3A_g + 3B_g + 3A_u + 3B_u.$$

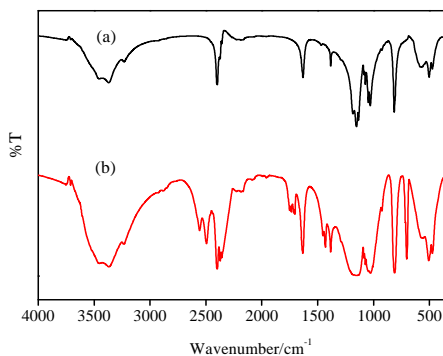


**Figure 6** Infrared spectrum of  $\text{Mn}(\text{H}_2\text{PO}_2)_2 \cdot \text{H}_2\text{O}$

(a) and its deuterated analogue (b).

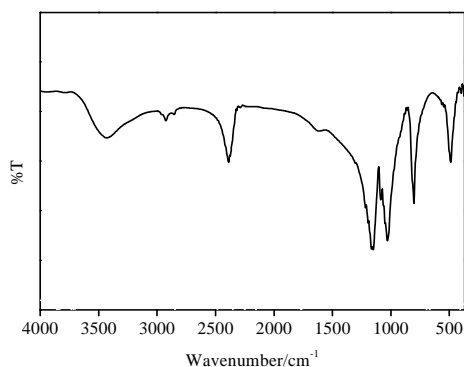


**Figure 7** Infrared spectrum of  $\text{Mn}(\text{H}_2\text{PO}_2)_2$  anhydrous.

The water molecules locate at  $C_1$  and  $C_1$  site symmetry. Under the selection rules of the  $C_1$  site group in the space group  $C_{2h}^5$ , the non degenerate  $\nu_1$ ,  $\nu_2$  and  $\nu_3$  vibrations are IR active transformed to an infrared active A mode. Thus, in the site group approximation, three bands should be expected in the infrared spectra. The correlation field splitting may cause additional splitting of A type vibration into four components. These type of vibrations are  $A_g$ ,  $B_g$ ,  $A_u$  and  $B_u$  modes. Consequently, six bands are expected to appear in both the infrared and Raman spectrum ( $A_g$  and  $B_g$  type modes are infrared inactive,  $A_u$  and  $B_u$  type modes are Raman inactive). In the case of  $C_1$  site

group, the correlation field splitting of types  $C_{2v}$ - $C_1$ - $C_{2h}$  for  $\text{H}_2\text{O}$  and  $\text{H}_2\text{PO}_2^-$  are illustrated in Table 2.

Three bands in the  $3460\text{-}3230\text{ cm}^{-1}$  region corresponding to the O-H stretching vibrations are seen in the infrared spectra of partially deuterated compound. Two bands appeared at  $2556$  and  $2495\text{ cm}^{-1}$  correspond to the uncoupled  $\nu_{\text{OD}}(\text{HOD})$ . The  $R_{\text{O}\dots\text{O}}$  distances were calculated from uncoupled  $\Delta\nu_{\text{OD}}(\text{HOD})$  by using following equation 3 and 4, respectively (Buanam-Om, 1981).

$$\Delta\nu_{\text{OD}}(\text{HOD}) = 2727 - \nu_{\text{OD,observed}}(\text{HOD}) \quad (3)$$

$$R_{\text{O}\dots\text{O}} = 3.748(\text{\AA}) - 0.178(\text{\AA}) \ln(\Delta\nu_{\text{OD}}(\text{HOD})/\text{cm}^{-1}) \quad (4)$$

The uncoupled  $\Delta\nu_{\text{OD}}(\text{HOD})$  are  $171$  and  $233\text{ cm}^{-1}$ , which correspond to  $R_{\text{O}\dots\text{O}}$  distances of  $2.833$  and  $2.778\text{ \AA}$ , respectively. The  $R_{\text{O}\dots\text{O}}$  distances of this compounds are classified as the strongly hydrogen bonds. The bending vibration of water molecules appear at  $1632\text{ cm}^{-1}$ . In this region appeared three new bands at  $1561$  (very weak),  $1471$  (weak, see in Fig. 8) and  $1384\text{ cm}^{-1}$  (medium), which are assigned to the overtone of  $\nu_2(A_1)\text{PH}_2$ , combination band and very low bending of water molecules, respectively. The band at  $1384\text{ cm}^{-1}$  is confirmed from the disappearance of this band in the anhydrous compound as shown in Figure 7. The bands at about  $3500\text{ cm}^{-1}$  are attributed to the moisture of instrument. The recent years, Šoptrajanov and co-worker (Šoptrajanov et al, 2004) reported the bending frequency at a very lower wavenumber in several solid hydrates. Two bands at  $1454$  and  $1432\text{ cm}^{-1}$  in the infrared spectrum of deuterated compounds are assigned to the bending of HOD molecules.

**Table 1** FTIR vibrational band positions ( $\text{cm}^{-1}$ ) at room temperature of  $\text{Mn}(\text{H}_2\text{PO}_2)_2 \cdot \text{H}_2\text{O}$  and its deuterated analogue ( $\text{Mn}(\text{H}_2\text{PO}_2)_2 \cdot \text{H}_2\text{O-dx}$ ).

Band positions( $\text{cm}^{-1}$ )		Assignments
$\text{Mn}(\text{H}_2\text{PO}_2)_2 \cdot \text{H}_2\text{O}$	$\text{Mn}(\text{H}_2\text{PO}_2)_2 \cdot \text{H}_2\text{O-dx}$	
3457 s	3459 s	$\nu_3(\text{B}_2)\text{H}_2\text{O}$
3369 s	3367 s	$\nu_1(\text{A}_1)\text{H}_2\text{O}$
3231 m	3236 m	$2\nu_2(\text{A}_1)\text{H}_2\text{O}$ or $\nu_1(\text{A}_1)\text{H}_2\text{O}$
-	2556 m, 2495 m	$\nu_3(\text{B}_2)\text{HOD}$
2398 s	2399 s	$\nu_1(\text{A}_1)\text{PH}_2$
2374 m, 2357 w	2373 s, 2357 s	$\nu_6(\text{B}_1)\text{PH}_2$
2267 w	-	$2\nu_9(\text{B}_2)\text{PH}_2$
2225 w	2228 w	$\nu_8(\text{B}_2)\text{PO}_2 +$ $\nu_3(\text{A}_1)\text{PO}_2$
2187, 2165 w	2187 w, 2167 w	$2\nu_7(\text{B}_1)\text{PH}_2$
-	2089 vw, 2068 vw	$2\nu_3(\text{A}_1)\text{PO}_2$
-	1752 m, 1736 m	$\nu_1(\text{B}_2)\text{HPD}$
-	1715 m, 1704 m	$\nu_6(\text{B}_2)\text{HPD}$
1632 s	1634 s	$\nu_2(\text{A}_1)\text{H}_2\text{O}$
1561 vw	-	$2\nu_2(\text{A}_1)\text{PH}_2$
-	1454 m, 1432 m	$\nu_2(\text{B}_2)\text{HOD}$
1471 w		$\nu_4(\text{A}_1)\text{PO}_2 +$ $\nu_3(\text{A}_1)\text{PO}_2$
1384 m	1384 m	$\nu_2(\text{A}_1)\text{H}_2\text{O}$
1291 m,sh	1292 m,sh	$2\nu_2(\text{A}_1)\text{PH}_2 +$ $\nu_4(\text{A}_1)\text{PO}_2$
1184,	-	$\nu_8(\text{B}_2)\text{PO}_2$
1154 vs, 1134 vs	1151 b	$\nu_9(\text{B}_2)\text{PH}_2$
1085 s, 1075 s	1086 s, 1075 s	$\nu_7(\text{B}_1)\text{PH}_2$
1048 vs, 1030 vs	1048 vs, 1028 vs	$\nu_3(\text{A}_1)\text{PO}_2$
926 w	926 w	$\nu_5(\text{A}_2)\text{PH}_2$
816 vs	813 vs	$\nu_2(\text{A}_1)\text{PH}_2$
-	703 s	$\nu_2(\text{B}_2)\text{HPD}$
583, 565 m	569 m	$\nu_4(\text{A}_1)\text{PO}_2$
503 s	506 s	$\nu_4(\text{A}_1)\text{PO}_2$
474 m	473 m	$\nu_4(\text{A}_1)\text{PO}_2$

### 3.2.2 $\text{NH}_4\text{MnPO}_4 \cdot \text{H}_2\text{O}$

The correlation table of this compound was presented by Stefov and co-worker (Stefov et al, 2004). One or two bands in the  $3481\text{-}3223\text{ cm}^{-1}$  region (Fig. 9) corresponding to the O-H stretching vibrations are observed in FTIR spectra of titled hydrate phosphate compounds. Three components with  $\text{A}_1$ ,  $\text{B}_1$  and  $\text{B}_2$  symmetries are expected under  $\text{C}_{2v}$  point group symmetry and  $\text{C}_s^{\text{yz}}$  site symmetry for this compound. The bands below  $3250\text{ cm}^{-1}$  in the FTIR spectra of the ammonium compounds are due to the N-H stretches and will not be discussed in the present paper.

The analysis of the vibrational spectra of the ammonium salts in the HOH bending vibrations is even more complicated than in the case of the hypophosphite compound, because understandably, bands due to bending vibrations of the ammonium ions also appear in the discussed spectral region. However, one band at  $1637\text{ cm}^{-1}$  is attributed to the  $\nu_2$  mode of water molecule of this compound. In  $\text{NH}_4\text{MnPO}_4 \cdot \text{H}_2\text{O}$ , the phosphate ion vibrations are found in the range of  $1008\text{-}931$ ,  $500\text{-}375$ ,  $1176\text{-}1015$  and  $630\text{-}510\text{ cm}^{-1}$  for  $\nu_1$ ,  $\nu_2$ ,  $\nu_3$  and  $\nu_4$ , respectively. In the region of symmetric stretching  $\nu_1(\text{A}_1)$  vibrations,  $\text{NH}_4\text{MnPO}_4 \cdot \text{H}_2\text{O}$  compound exhibits two bands at about  $956$  and  $940\text{ cm}^{-1}$  (Fig.10). While, in the region of the triply degenerate asymmetric stretching  $\nu_3(\text{F}_2)$  mode appears three bands, which indicate the distortion from  $\text{T}_d$  symmetry of  $\text{PO}_4^{3-}$  unit. Similarly, the splitting of the degenerate asymmetric bending  $\nu_4$  vibrations is observed in two bands (Fig.10).

**Table 2** The unit-cell group analysis for the three internal water modes (a) and hypophosphite anion (b).

(a) Water molecule internal vibrations			
Mode	Molecular point group	Site group	Factor group
	$C_{2v}$	$C_1$	$C_{2h}$
$V_1, V_2$	$A_1$	$A_g(3)$	$A_g(3)$ $B_g(3)$
$V_3$	$B_2$	$A_u(3)$	$A_u(3)$ $B_u(3)$
	$C_{2v}$	$C_i$	$C_{2h}$
$V_1, V_2$	$A_1$	$A_g(3)$	$A_g(3)$ $B_g(3)$
$V_3$	$B_2$	$A_u(3)$	$A_u(3)$ $B_u(3)$
(b) Hypophosphite anion vibrations			
Mode	Molecular point group	Site group	Factor group
	$C_{2v}$	$C_1$	$C_{2h}$
$V_1-V_4$	$A_1(4)$	$A_g(9)$	$A_g(9)$ $B_g(9)$
$V_5$	$A_2(1)$	$A_u(9)$	$A_u(9)$ $B_u(9)$
$V_6, V_7$	$B_1(2)$	$A_g(9)$	$A_g(9)$ $B_g(9)$
$V_8, V_9$	$B_2(2)$	$A_u(9)$	$A_u(9)$ $B_u(9)$
	$C_{2v}$	$C_i$	$C_{2h}$
$V_1-V_4$	$A_1(4)$	$A_g(9)$	$A_g(9)$ $B_g(9)$
$V_5$	$A_2(1)$	$A_u(9)$	$A_u(9)$ $B_u(9)$
$V_6, V_7$	$B_1(2)$	$A_g(9)$	$A_g(9)$ $B_g(9)$
$V_8, V_9$	$B_2(2)$	$A_u(9)$	$A_u(9)$ $B_u(9)$

Isotopic dilution technique was applied to the hydrogen bonding study in solid hydrates. FT-IR and FT-Raman spectra of deuterated samples containing small amount of HOD molecules surrounded by a large amount of  $D_2O$  (as in our study) or  $H_2O$  exhibit the uncoupled  $\nu_{OH}(HOD)$  or  $\nu_{OD}(HOD)$ . That means, the intermolecular and

intramolecular coupling between water molecules are eliminated.

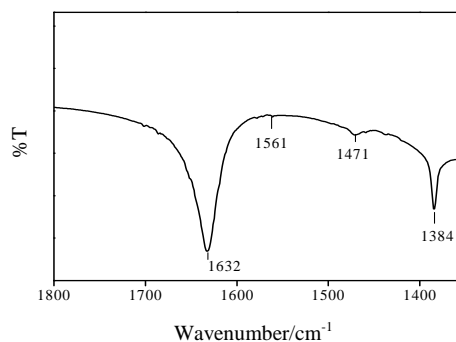


**Figure 8** Infrared spectrum of  $Mn(H_2PO_2)_2 \cdot H_2O$  in the  $1800-1300 \text{ cm}^{-1}$  region.

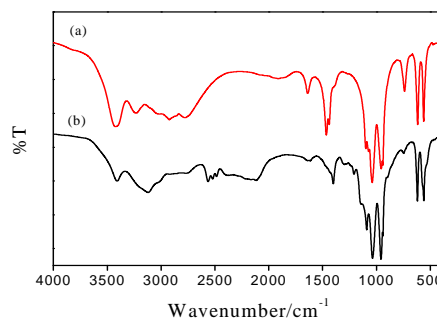


**Figure 9** Infrared spectrum of  $NH_4MnPO_4 \cdot H_2O$  (a) and its deuterated analogue (b) in the region of  $4000-370 \text{ cm}^{-1}$ .

The observed frequency is called the “uncoupled” one. In this paper, the uncoupled  $\nu_{OH}(HOD)$  was studied. The FT-IR band positions of isolated HOD molecule according to the effective site symmetry  $C_s$  are the stretching vibrations  $\nu_{OD}(A')$  at  $2727$ ,  $\nu_2(\delta)$  at  $1402$  and  $\nu_{OH}(A'')$  at  $3707 \text{ cm}^{-1}$ . The uncoupled  $\nu_{OH}(HOD)$  of ammonium salts show complicated peaks in the region of the HOD stretching vibration. Thus the uncoupled  $\nu_{OH}(HOD)$  of this compounds is not clearly observed, for appearing as coupled vibrations.



### 3.2.3 The librational modes of water molecules

In this region, the intensity of librational modes of water in infrared spectrum of hypophosphite compound are weaker than those of hypophosphite anion. Two vibrational modes of this anion are observed in the same region. Thus the coupling vibrations exist in this region. However, the wagging libration of  $\text{NH}_4\text{MnPO}_4 \cdot \text{H}_2\text{O}$  compound can be clearly observed at  $740 \text{ cm}^{-1}$  (Fig. 10c).

### 3.2.4 Vibrations of the $\text{H}_2\text{PO}_2^-$ ions

The hypophosphite compound studies in this work crystallizes in the space group  $C_{2h}^5$ , with  $Z=4$ . The hypophosphite site symmetry group is  $C_1$ . The reduction formula used to calculate the number of fundamental frequencies of each species have been followed by Ferraro and Ziomek (Ferraro & Ziomek, 1975) as given in the following equations :

$$N_i = 1/N_G \sum n_c \Xi(R) \chi_i(R) \quad (5)$$

Where  $\Xi(R) = (\mu_R - 2)(1 + 2\cos\phi)$  for proper rotations, and  $\Xi(R) = (\mu_R)(-1 + 2\cos\phi)$  for improper rotations ;  $\mu_R$  is the number of atoms invariant under the symmetry operation R,

The angle  $\phi$  is associated with the proper or improper rotation R. The negative sign is used with the improper rotation, such as in the case of  $\sigma_d$ ,  $\sigma_v$  or  $S_2$ . The positive sign is used with the proper rotation, such as in the case of E or  $C_2$ . These values are summarized in Table 3.

The number of fundamentals of  $\text{H}_2\text{PO}_2^-$  ions can be carried out and summarize to be:

$$\Gamma(\text{vib}, \text{H}_2\text{PO}_2^-) = 4A_1 + A_2 + 2B_1 + 2B_2$$

The determination of the allowed vibrations in the infrared can be calculated by using equation(6).

$$N_i = 1/N_G \sum n_c \chi_M(R) \chi_i(R) \quad (6)$$

Where,  $N_G$  = the number of element in the group (e.g.,  $C_{2v}$ :  $1E + 1C_2 + 2\sigma_v = 4$ ),

$n_c$  = the number of elements in each class,

$\chi_M(R)$  = the character of the dipole moment;

$\chi_M(R) = \pm 1 + 2\cos\phi$ ,

$\chi_i(R)$  = the character of the vibration species.

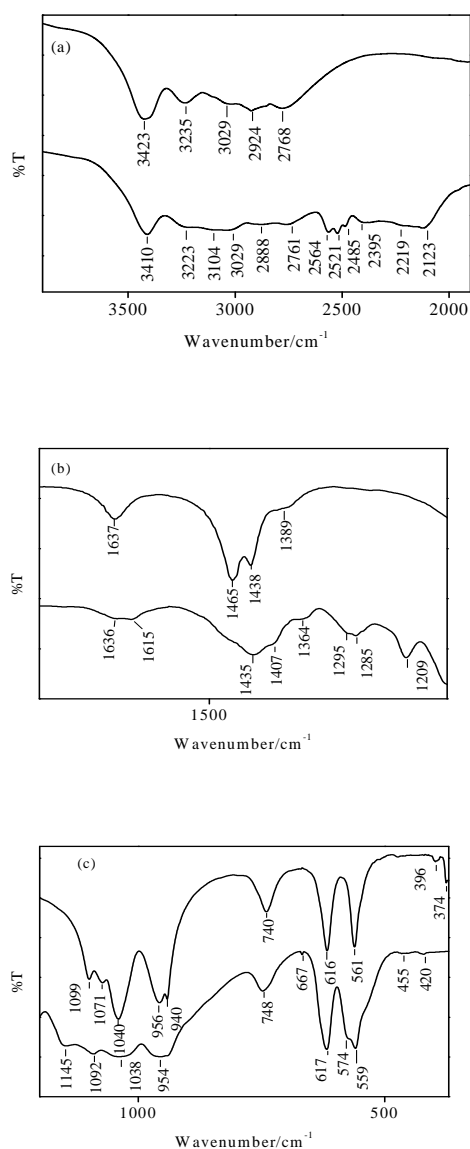


**Figure 10** Comparison the FTIR spectra between  $\text{NH}_4\text{MnPO}_4 \cdot \text{H}_2\text{O}$  (upper curve) and its deuterated analogue (lower curve) in three regions.

The calculation for the isolated hypophosphite anion results nine modes of vibration, all of which are non-degenerate (see in Table 2b) and all modes are Raman and infrared active except for the  $A_2$  mode which is infrared inactive. The selection rules for the hypophosphite at  $C_1$  site in the Bravais cell, 16 infrared [ $A_u(8) + B_u(8)$ ] and 18 Raman [ $A_g(9) + B_g(9)$ ] bands are expected. The coupling of these modes with the appropriate vibrations of other molecules at each sites in the unit cell will further causes the complicate vibrational spectra.

**Table 3** Character Table for  $C_{2v}$  Symmetry of hypophosphite anion (Ferraro & Ziomek, 1975).

$C_{2v}$	E	$C_2$	$\sigma_v$ (xz)	$\sigma_v$ (yz)	
$A_1$	1	1	1	1	$\chi_i(R)$
$A_2$	1	1	-1	-1	
$B_1$	1	-1	1	-1	
$B_2$	1	-1	-1	1	
$\varphi$	$0^\circ$	$180^\circ$	$0^\circ$	$0^\circ$	$\chi_M(R)$
$2 \cos \varphi$	2	-2	2	2	
$\pm 1 + 2 \cos \varphi$	3	-1	1	1	
$\mu_R$	5	1	3	3	e.g., $H_2PO_2^-$
$\Xi(R)$	9	1	3	3	

Three bands in the region of 2450-2300  $cm^{-1}$  (non deuteration sensitive bands) are seen in both protiated and deuterated compounds (Fig. 6), which attributed to stretching of  $PH_2$  mode.

Four bands (Fig. 11a) at 1752, 1736, 1715 and 1704  $cm^{-1}$  are attributed to the uncoupled [ $\nu_1(B_2)$  HPD], [ $\nu_1(B_2)$  HPD], [ $\nu_6(B_2)$  HPD] and [ $\nu_6(B_2)$  HPD], respectively. The vibrational modes of [ $\nu_3(A_1)$   $PO_2$ ], [ $\nu_6(B_1)$   $PH_2$ ], [ $\nu_7(B_1)$   $PH_2$ ] and [ $\nu_9(B_2)$   $PH_2$ ] appear two bands in both non-deuterated and deuterated compounds, which correspond to unit-cell group or correlation field splitting analysis (see Table 2). The presentation in Table 2, both  $A_1$ ,  $B_1$  and  $B_2$  modes

should exhibit 2 bands, which infrared active. However, the vibrational mode of [ $\nu_3(A_1)$   $PO_2$ ] appear 4 bands at 583, 565, 503 and 474  $cm^{-1}$ , which is not agree with unit-cell group analysis. This observation can be described to be due to the lowering site symmetry of the hypophosphite anion in the lattice which enable the forbidden modes in the IR spectra can be observed. Additional complication of the IR spectra is caused by the observation of correlation and overtone bands as well as the effect of Fermi resonance. The vibrational band positions of hypophosphite anion (Fig. 11b) are summarized in

Table 1.

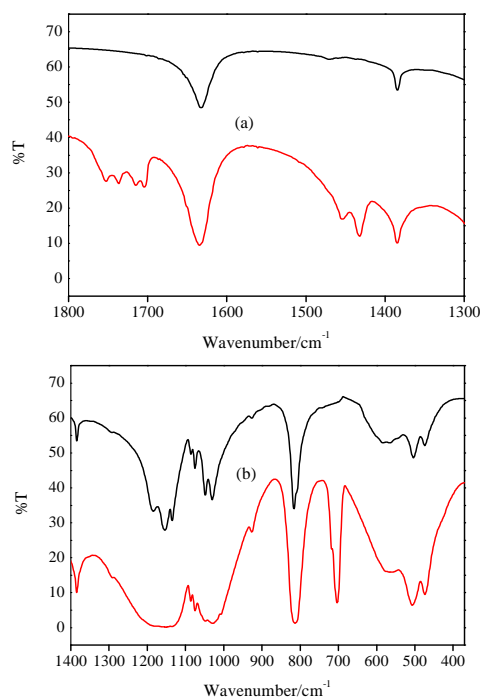


**Figure 11** Infrared spectrum of  $Mn(H_2PO_2)_2 \cdot H_2O$  (upper curve) and its deuterated analogue (lower curve) in the region of (a)  $H_2O$  bending and (b)  $H_2PO_2^-$  anion vibrations.

#### 4. Conclusions

Thermal gravimetric analysis (TGA) and differential scanning calorimetry (DSC) were used to study the thermal decomposition of a synthetic

manganese hypophosphite and phosphate compounds. Manganese hypophosphite compound was stable up to 120 °C, then the dehydration occurs at 140 °C followed by the decomposition of this compound at 360 °C. While, the manganese phosphate compound was stable up to 190 °C followed by a slow transition to  $\text{MnHPO}_4$  and  $\text{Mn}_2\text{P}_2\text{O}_7$ . The results of two methods (TG and DSC) agree well with each other. The final product from the calcination of two compounds was  $\text{Mn}_2\text{P}_2\text{O}_7$ , which is the simple route to produce the manganese pyrophosphate.

Fourier transform infrared spectra of both protiated and deuterated compounds showed a new band at  $1384\text{ cm}^{-1}$  for manganese hypophosphite, which have not been reported elsewhere in the hypophosphite compounds. This new band was attributed to the very low bending of the water molecules. The infrared spectra of deuterated compound, the uncoupled  $\nu_{\text{OD}}(\text{HOD})$  appear at 2556 and  $2494\text{ cm}^{-1}$ , the frequency shifts,  $\Delta\nu_{\text{OD}}(\text{HOD})$  of 171 and  $233\text{ cm}^{-1}$  correspond to  $R_{\text{O}\dots\text{O}}$  distances of 2.833 and  $2.778\text{ cm}^{-1}$ , respectively. The hydrogen bond strengths in these compounds were classified as the strong ones.

## 5. Acknowledgements

The authors would like to thank the Department of Chemistry, Faculty of Science, Khon Kaen University for providing laboratory facilities. Development and Promotion in science and Technology Talents Project(DPST) and Center for Innovation Chemistry:Postgraduate Education and Research in Chemistry (PERCH-CIC) for the financial support.

## 6. References

- Basset H and Bedwell WL. 1993. *J. Chem. Soc.*, 137.
- Bian JJ, Kim DW and Hong KS. 2003. Microwave dielectric properties of  $\text{Ca}_2\text{P}_2\text{O}_7$ . *J. Eur. Ceram. Soc* 23:2589-92.
- Boonchom B, Youngme S, Maensiri S and Danvirutai C. 2007. Nanocrystalline serrabrancaite ( $\text{MnPO}_4\cdot\text{H}_2\text{O}$ ) prepared by a simple precipitation route at low temperature. *J. Alloys. Compds.* Inpress.
- Buanam-Om C. 1981. Raman and Infrared Spectroscopic Study of the Structure of Water ( $\text{H}_2\text{O}$ , HOD,  $\text{D}_2\text{O}$ ) in Stoichiometric Crystalline Hydrates and in Electrolyte Solutions. Ph.D. Dissertation, Mauersberger, Marburg, Germany.
- Carling SG, Day P and Visser D. 1995. Crystal and magnetic structures of layer transition metal phosphate hydrates. *Inorg. Chem* 34:3917-27.
- Chung UC, Mesa JL, Pizarro JL, Jubera V, Lezama L, Arriortua MI and Rojo T. 2005.  $\text{Mn}(\text{HPO}_3)$ : A new manganese (II) phosphite with a condensed structure. *J. Solid. State. Chem* 178:2913-21.
- Danvirutai C, Amornraksa K, Puengpan N, Chunchartprasert L, Jernsawatdipong P, Arunin S, Pooisittisak S, Rothanavibhata S, Srithanratana T and Patrick WH. 1989. Technology Development for Reclamation of Salt Affected Areas in Northeast Thailand, 12.
- Ferraro JR and Ziomek JS. 1975. Introductory Group Theory and Application to Molecular Structure. Plenum Press, New York and London.

- Julien CM, Salah AA, Gendron F, Morhange JF, Mauger A and Ramana CV. 2006. Microstructure of  $\text{LiXPO}_4$  (X = Ni, Co, Mn) prepared by solid state chemical reaction *Scripta Materialia* 55:1179-82.
- Liu R, Moody PR, Vanburen AS, Clark JA, Krauser JA and Tate DR. 1996. On assignment of fundamental vibrational modes of hypophosphite anion and its deuterated analogue. *Vibrational Spectroscopy* 10:325-9.
- Marcos MD, Amoros F, Sapiña F and Beltrán D. 1992. Crystal structure and magnetic properties of  $\alpha$ -  $\text{Mn}(\text{H}_2\text{PO}_2)_2 \cdot \text{H}_2\text{O}$ . *J. Alloys. Compds* 188:133-7.
- Marincean S, Custelcean R, Jackson JE and Stein RS. 2005. Structure reinvestigation of ammonium hypophosphite. *Inorg. Chem* 44:45-8.
- Onoda B, Nariai H, Moriwaki A, Maki H and Motooka I. 2002. Formation and catalytic characterization of various rare earth phosphates. *J. Mater. Chem* 12:1754-60.
- Onoda H, Kojima K and Nariai H. 2006. Additional effects of rare earth elements on formation and properties of some transition metal pyrophosphates. *J. Alloys. Compds* 408:568-72.
- Onoda H, Ohta T and Kojima K. 2006. Mechanochemical reforming of nickel pyrophosphate. *Mater. Chem. Phys* 98:363-7.
- Onoda H., Nariai H, Maki H and Motooka I. 2001. *Phosphorus Res. Bull* 12:139.
- Onoda H, Nariai H, Maki H and Motooka I. 1999. *Phosphorus Res. Bull* 9:69.
- Oxy Occidental Chemical Corporation Specialty Business Group, Hypo Products Handbook, <http://www.erowid.org/archive/rhodium/pdf/hypophosphoric.pdf>
- Smaalen S van, Dinnebier R, Hanson J, Gollwitzer J, Büllfeld F, Prokofiev A and Assmus W. 2005. High-temperature behavior of vanadyl pyrophosphate  $(\text{VO})_2\text{P}_2\text{O}_7$ . *J. Solid. State. Chem* 178:2225-30.
- Šoptrajanov B, Stefov V, Kuzmanovski I, Jovanovski G, Lutz HD and Engelen B. 2002. Very low H-O-H bending frequencies. IV. Fourier transform infrared spectra of synthetic dittmarite. *J. Mol. Struct* 613:7-14.
- Šoptrajanov B, Jovanovski G, Pejov L and Stefov V. 2004. *J. Mol. Struct* 706:101.
- Stefov V, Šoptrajanov B, Spirovski F, Kuzmanovski I, Lutz HD and Engelen B. 2004. Infrared and Raman spectra of magnesium ammonium phosphate hexahydrate (struvite) and its isomorphous analogues. *J. Mol. Struct* 689:1-10.
- Tanner PA, Yu-Long L and Mak, TCW. 1997. Synthesis, crystal structures and vibrational spectra of zinc hypophosphites. *Polyhedron* 16:495-05.
- Tanner PA, Faucher MD and Mak TCW. 1999. Synthesis, structure, and spectroscopy of rare earth hypophosphites. 1. An hydrous and monohydrated lanthanide hypophosphites. *J. Inorg. Chem* 38:6008-23.
- Zachariasen WH, and Mooney RCL. 1934. *J. Chem. Phys* 2:34.